



Synthesis, characterization, antibacterial, and antifungal activities of one-dimensional O–H...O hydrogen-bonded Cu(II) and Ni(II) complexes

S. Celen, E. Gungor, H. Kara & A. D. Azaz

To cite this article: S. Celen, E. Gungor, H. Kara & A. D. Azaz (2016) Synthesis, characterization, antibacterial, and antifungal activities of one-dimensional O–H...O hydrogen-bonded Cu(II) and Ni(II) complexes, *Molecular Crystals and Liquid Crystals*, 631:1, 164-175, DOI: [10.1080/15421406.2016.1170284](https://doi.org/10.1080/15421406.2016.1170284)

To link to this article: <http://dx.doi.org/10.1080/15421406.2016.1170284>



Published online: 12 Jul 2016.



Submit your article to this journal [↗](#)



Article views: 33



View related articles [↗](#)



View Crossmark data [↗](#)

Synthesis, characterization, antibacterial, and antifungal activities of one-dimensional O—H...O hydrogen-bonded Cu(II) and Ni(II) complexes

S. Celen^a, E. Gungor^b, H. Kara^{b,c}, and A. D. Azaz^d

^aFaculty of Science and Art, Department of Molecular Biology and Genetic, Balıkesir University, Balıkesir, Turkey;

^bFaculty of Science and Art, Department of Physics, Balıkesir University, Balıkesir, Turkey; ^cFaculty of Science, Department of Physics, Mugla Sıtkı Koçman University, Mugla, Turkey; ^dFaculty of Science and Art, Department of Biology, Balıkesir University, Balıkesir, Turkey

ABSTRACT

Two Schiff base complexes, [Cu(HL)₂], **1** and [Ni(HL)₂], **2** [H₂L = 2-((E)-(2-hydroxyethylimino)methyl)-1-naphthol] have been synthesized and characterized by elemental analysis, ¹H NMR, ¹³C NMR, IR spectroscopy, and X-ray diffraction. In the crystalline architecture of **1** and **2**, intermolecular O—H...O hydrogen bonds link the molecules which form one-dimensional polymeric chain structure along the *c* axis. C—H...O and C—H... π intermolecular interaction also connect the molecules in the structures which form to 3D structures of **1** and **2**. The ligand and metal complexes **1** and **2** were screened for antibacterial and antifungal activities.

KEYWORDS

Antibacterial activity;
Antifungal activity; Schiff
base; Single crystal X-ray


1. Introduction

Schiff bases and their metal complexes have attracted considerable attention owing to their physicochemical properties and biological activities [1–3]. These complexes have been widely studied in medicinal and pharmaceutical field as the antibacterial, antifungal, and antiviral agents [4–6]. Therefore the discoveries of effective antibacterial and antifungal drugs have become an urgent task for infectious diseases [7]. Many drugs possess modified toxicological and pharmacological properties when they are in the form of the metal complexes. These reason encouraged us to investigate the coordination chemistry of the Schiff bases metal complexes in an attempt to examine the modes of binding in the solid state and to study biological activity [8, 9].

Recently, our research group and others have reported the structural characterization and the biological properties of ONNO, ONO, and NNN donor-type Schiff-base metal complexes [10–15]. In view of the importance of Cu(II) and Ni(II) compounds and our interest in the chemistry of coordination compounds involving chelating Schiff bases and in an effort to enlarge the library of such complexes, we report herein the characterization and antibacterial

CONTACT S. Celen  selcelen@yahoo.com

Color versions of one or more of the figures in the article can be found online at www.tandfonline.com/gmcl.

 Crystallographic data for the structure reported in this paper have been deposited with the Cambridge Crystallographic Data Centre (The Director, CCDC, 12 Union Road, Cambridge, CB2 1EZ, UK; e-mail: deposit@ccdc.cam.ac.uk; <http://www.ccdc.cam.ac.uk>; fax: +44 1223 336033) and are available free of charge on request, quoting the Deposition No. CCDC **865487** and **865488**.

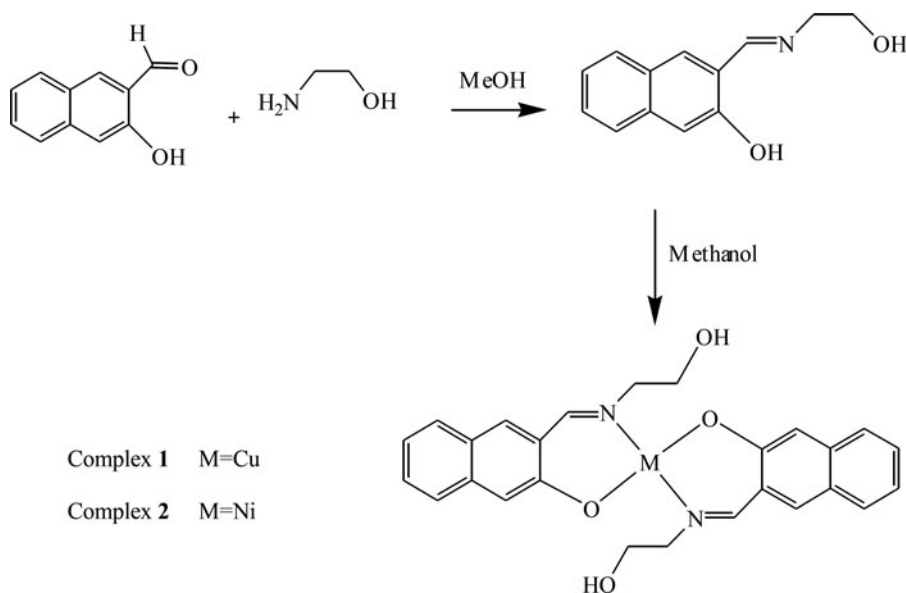
© 2016 Taylor and Francis Group, LLC

and antifungal properties of H_2L and $[\text{Cu}(\text{HL})_2]$, **1** and $[\text{Ni}(\text{HL})_2]$, **2** against the 10 bacteria, 2 yeast, 5 filamentous fungi.

2. Experimental

2.1. Materials and physical measurements

All chemical reagents and solvents were purchased from Merck or Aldrich and used without further purification. Elemental (C, H, N) analyses were carried out by standard methods with a LECO, CHNS-932 analyzer. Infrared spectra (KBr pellets) were obtained on a *FT-IR* Perkin-Elmer Model Bx 1600 instrument. ^1H and ^{13}C NMR spectra of the H_2L ligand were recorded in (DMSO) on a Bruker Biospin (300 MHz). The complexes **1** and **2** were prepared by different synthetic procedure compared to previously reported complexes [16]. The synthetic route of the ligand H_2L , complex **1** and **2** are outlined in Scheme 1.



Scheme 1. The synthetic route of H_2L , **1** and **2**.

2.2. Synthesis of H_2L ligand

The tridentate Schiff base ligand H_2L was prepared by mixing 2-hydroxy-1-naphthaldehyde (1 mmol) and ethanolamine (1 mmol) with the molar ratio of 1:1 in hot methanol (50 cm³). The solution obtained was stirred at 65°C for 30 min. The yellow compound has precipitated from solution on cooling. H_2L : Yellow compound, yield 80%; Anal. Calcd. for $\text{C}_{13}\text{H}_{13}\text{NO}_2$ (%): C, 72.54; H, 6.09; N, 6.51. Found (%): C, 72.49; H, 6.07; N, 6.52%. ^1H NMR (DMSO, δ ppm): 3.465–3.890, H_{alif} , 4H. 5.090, $\text{H}_{\text{alcoholic}}$, 1H. 6.710–8.100, H_{Ar} , 6H. 9.075, H_{imm} , 1H. 13.910, $\text{H}_{\text{phenolic}}$, 1H. ^{13}C NMR (DMSO, δ ppm): 53.49 (–N–CH₂–), 60.79 (–HO–CH₂–), 159.73 (–C–COH), 178.79 (–C=N–). IR (KBr) cm^{–1}: $\nu(\text{O–H})$ 3162, $\nu(\text{C=N})$ 1643.

2.3. Synthesis of complex 1 and 2

Complex **1** was prepared by addition of copper(II) acetate monohydrate (0.199 g, 1 mmol) in 30 cm³ of hot methanol to the ligand (**H₂L**) (1 mmol) in 30 cm³ of hot methanol. This solution was warmed to 65°C and stirred for 15 min. A green-colored solution was obtained and then left to evaporate in the room temperature. Several weeks of standing were led to the growth of green-colored crystals. Complex **2** was prepared in a similar way using nickel(II) acetate tetrahydrate (0.248 g, 1 mmol) in hot methanol.

Complex **1**: Green crystals, yield 75%. Anal. Calcd. for C₂₆H₂₄CuN₂O₄(%): C, 63.47; H, 4.92; N, 5.69. Found (%): C, 63.65; H, 4.49; N, 5.68%. The IR (KBr) (cm⁻¹): $\nu(\text{O-H})$ 3372, $\nu(\text{C=N})$ 1613.

Complex **2**: Brown crystals, yield 75%. Anal. Calcd. for C₂₆H₂₄NiN₂O₄(%): C, 64.10; H, 4.97; N, 5.75. Found (%): C, 64.08; H, 4.98; N, 5.71%. The IR (KBr) (cm⁻¹): $\nu(\text{O-H})$ 3389, $\nu(\text{C=N})$ 1640.

2.4. X-ray structure determination

Diffraction measurements were made on a Bruker ApexII kappa CCD diffractometer using graphite monochromated MoK α radiation ($\lambda = 0.71073$ Å) at 100 K for **1** and **2**. The intensity data were integrated using the APEXII program [17]. Absorption corrections were applied based on equivalent reflections using SADABS [18]. The structures were solved by direct methods and refined using full-matrix least-squares against F^2 using SHELXL [19]. All nonhydrogen atoms were assigned anisotropic displacement parameters and refined without positional constraints. Hydrogen atoms were included in idealized positions with isotropic displacement parameters constrained to 1.2 times the U_{equiv} of their attached carbon atoms. There is disorder in the ethanolamine portion of the ligand for **2**. The O4 atom was split into the O4A and O4B with 81% and 19% occupancy, respectively. The Level B Alerts of **2** result from disordered atom O4. Residual density is located 0.714 Å from atom O4B which was refined isotropically due to its high thermal motion and it was difficult to model reliable positions. The absolute configuration of the enantiomer present in the crystal selected for data collection was established by means of the Flack x parameter [20], although this has no chemical significance. The Flack x parameters were 0.45(2) for **1** and 0.45(4) for **2** calculated using 597 for **1** and 538 for **2** quotients of type $[(I^+) - (I^-)] / [(I^+) + (I^-)]$ [21]. Use of the TWIN/BASF instructions in SHELXL [19] gave a value for the twin fraction of 0.45 for **1** and **2**. For compounds **1** and **2**, the value of the Flack x parameter gives evidence of the partial inversion twinning.

All of the crystallographic computations were carried out using SHELXTL [19], ORTEP II [22], and MERCURY [23] programs. The crystallographic data, conditions used for the intensity data collection and some features of the structure refinement are listed in Table 1. Selected bond lengths and angles for the complexes are given in Table 2. Ortep diagrams of **1** and **2** are shown in Fig. 1, while Mercury packing diagrams are displayed in Figs. 2 and 3.

2.5. Biological activity

The ligand **H₂L** and the metal complexes **1** and **2** were subjected to screening for antimicrobial activity by using agar disc diffusion assay, microdilution broth assay and single spore culture

Table 1. Crystal data and structure refinement for **1** and **2**.

	1	2
Chemical Formula	$C_{26}H_{24}CuN_2O_4$	$C_{26}H_{24}NiN_2O_4$
Formula weight ($g\ mol^{-1}$)	492.01	487.18
Crystal system	Monoclinic	Monoclinic
Space group	$P2_1$	Cc
Unit cell dimensions	$a = 5.4701(2)\ \text{\AA}$ $\alpha = 90^\circ$ $b = 17.0068(7)\ \text{\AA}$ $\beta = 94.39(2)^\circ$ $c = 11.2954(4)\ \text{\AA}$ $\gamma = 90^\circ$	$a = 22.0413(15)\ \text{\AA}$ $\alpha = 90^\circ$ $b = 10.1917(7)\ \text{\AA}$ $\beta = 107.76(3)^\circ$ $c = 9.9155(7)\ \text{\AA}$ $\gamma = 90^\circ$
$V / \text{\AA}^3$	1047.72(7)	2121.2(3)
Z	2	4
$\rho_{\text{calc}} / g\ cm^{-3}$	1.560	1.525
μ / mm^{-1}	1.081	0.953
Temperature (K)	100(2)	100(2)
Reflections collected	9896	14228
Independent reflections	4621	2466
Goodness-of-fit on F^2	1.112	1.106
R indices [$I > 2\sigma(I)$]	$R_1 = 0.0212$, $wR_2 = 0.0540$	$R_1 = 0.0433$, $wR_2 = 0.1098$
Flack Parameter	0.45(2)	0.45(4)

Table 2. Some selected bond lengths [\AA] and angles [$^\circ$] for **1** and **2**.

Bond lengths	1		2
Cu1–O1	1.889(2)	Ni1–O1	1.851(3)
Cu1–O2	1.905(2)	Ni1–O2	1.820(3)
Cu1–N1	1.997(2)	Ni1–N1	1.889(3)
Cu1–N2	2.001(2)	Ni1–N2	1.906(3)
N1–C24	1.298(3)	N1–C1	1.301(5)
N2–C11	1.298(3)	N2–C22	1.297(4)
N1–C25	1.480(3)	N1–C23	1.482(5)
N2–C12	1.483(3)	N2–C24	1.469(5)
Bond angles			
O1–Cu1–O2	175.10(8)	O1–Ni1–O2	176.25(13)
O1–Cu1–N1	89.13(8)	O1–Ni1–N1	89.00(14)
O1–Cu1–N2	90.94(8)	O1–Ni1–N2	90.98(13)
O2–Cu1–N1	90.81(8)	O2–Ni1–N1	92.11(14)
O2–Cu1–N2	89.39(8)	O2–Ni1–N2	87.99(13)
N1–Cu1–N2	176.78(9)	N1–Ni1–N2	178.88(13)

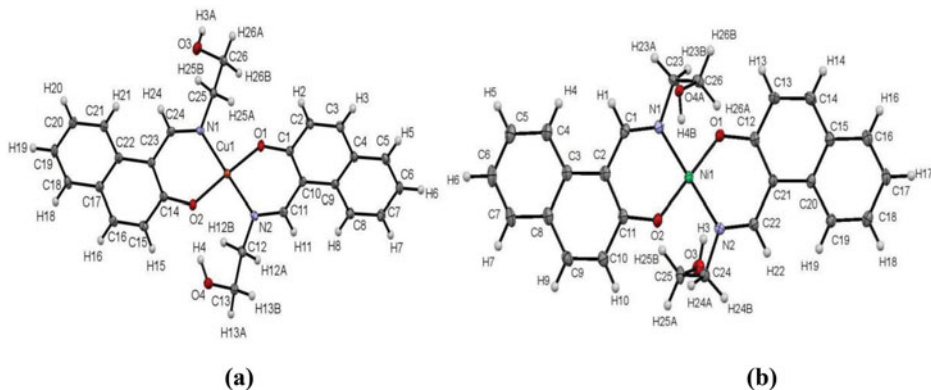


Figure 1. (a) The molecular structure of complex **1**. (b) The molecular structure of complex **2**. Displacement ellipsoids are drawn at 50% probability.

technique (for filamentous fungi) [24–26]. The antimicrobial activity of the ligand **H₂L** and its metal complexes **1** and **2** were evaluated against ten bacteria, two yeast, and five filamentous fungi (The tested microfungi were isolated from soil in our Department).

2.5.1. Agar disc diffusion method

The agar disc diffusion method was employed for the determination of antimicrobial capacities of the ligand **H₂L** and the metal complexes **1** and **2**. Briefly, a suspension of the tested microorganism (500 μ L of 10^8 CFU/mL) was spread on the solid media plates. Each test solution (1000 μ g/mL) was prepared in DMF. Then filter paper discs (6 mm in diameter) were soaked with 20 μ L of the stock solutions and placed on the inoculated plates. After keeping at 2°C for 2 h, they were incubated at 37°C for 24 h for bacteria and *Candida albicans* (*Campylobacter jejuni* was incubated at 42°C, microaerophilic conditions for 48 h). The diameter of the inhibition zones were measured in millimeters. Each test was carried out in triplicate and the average value was calculated for inhibition zone diameters.

2.5.2. The microdilution broth method

A microdilution broth susceptibility assay was used for determination of Minimum Inhibitory Concentration (MIC) [25]. Serial dilutions of compounds were prepared in sterile distilled water in 96-well plates. Freshly grown bacterial suspension was standardized to 10^8 CFU/mL (McFarland no. 0.5) in double-strength Mueller–Hinton broth (*Listeria monocytogenes* in Buffered Listeria Enrichment Broth and yeast suspension of *Candida albicans* in Saboraud Dextrose Broth). Sterile distilled water was served as growth control. 100 μ L of each microbial suspension were then added to each well. The last row containing only the serial dilutions of antibacterial agent without microorganism was used as negative control. After incubation at 37°C for 24 h (*Campylobacter jejuni* was incubated at 42°C microaerophilic conditions for 48 h), the first well without turbidity was determined as the minimal inhibitory concentration. Chloramphenicol (1000 μ g/mL) and Ketoconazole (1000 μ g/mL) were served as positive controls. Each test was performed in triplicate.

2.5.3. Antifungal studies

In order to obtain conidia, the fungi was cultured on Czapek Dox Agar and Malt Extract Agar medium (Merck) in 9 cm petri dishes at 25°C for 7–10 days. Harvesting was carried out by suspending the conidia in a 1% (w/v) sodium chloride solution containing 5% (w/v) DMSO. The spore suspension was then filtered and transferred into tubes and stored at –20°C [27]. The 1 mL spore suspension was taken and diluted in a loop drop until one spore could be captured. One loop drop from the spore suspension was applied onto the centre of the petri dish containing Czapek Dox Agar and Malt Extract Agar. 20 μ L of each complex was applied onto sterile paper discs (6 mm in diameter) and placed in the petri dishes and incubated at 25°C for 72 h. Spore germination during the incubation period was followed using a microscope (Olympus BX51) in 8-h intervals. The inhibition of fungal growth was measured using the following equation [28].

$$\text{Inhibition \%} = 100 \times \frac{C - T}{C}$$

where C is the diameter of fungal growth on the control, T is the diameter of fungal growth on the test plate. The activities of the complexes were compared with the activity of standard antifungicide ketoconazole.

3. Results and discussion

3.1. X-ray structure of **1** and **2**

The crystal structure of **1** was previously reported at room temperature [29]. We report here a redetermination of **1** at 100 K, with improved precision. The precision of the unit-cell dimensions of **1** was improved by an order of magnitude. The unit-cell volume decreased by *ca* 24.11 Å³ for **1** [16]. The structure of **2** was previously reported in triclinic symmetry (space group *P*-1) at room temperature [16]. The present study re-determines of **2** with monoclinic symmetry (space group *Cc*) at 100 K.

The complex **1** and **2** crystallizes in chiral space groups *P*2₁ and *Cc*, respectively. The asymmetric unit consists of a monomeric [Cu(HL)₂] unit for **1** and a monomeric [Ni(HL)₂] unit for **2**. The crystal structure of **2** was previously reported in the triclinic symmetry (space group *P*-1) at room temperature, its asymmetric unit consists of half each of two independent molecules which have similar geometries, with the Ni atom of each of the two neutral complex molecules lying on an inversion centre [16]. The present study re-determines of **2** with monoclinic symmetry (space group *Cc*) at 100 K. The asymmetric unit consists of one molecule and has glide planes since space group *Cc*. Re-determine structure of **2** has the different molecular structure and packing since the different space group.

The metal atom is coordinated by two bidentate Schiff base ligands through two N and two O atoms in a mutual *trans* disposition, where the Schiff base (H₂L) is a deprotonated monoanionic ligand. Alcoholic O atoms of the ligand do not coordinate to the central metal ions in **1** and **2**. The O-M-O and N-M-N angles are close to 180. Therefore, the geometry of the metal ion is square planar, as has been observed previously reported ones [16, 29]. The mean deviation of the plane formed by Cu^{II} and Ni^{II} ions and the four coordination atoms (N1, N2, O1, O2) are 0.013 Å and 0.016 Å, respectively, and metal atom lies in the center of the plane. The bond lengths and bond angles are in the ranges observed for previously reported and similar systems [16, 29, 30].

Intermolecular O—H...O hydrogen bonds and C—H... π interactions are shown very shortly in previously reported systems [16, 29]. So we give detailed hydrogen bonding motifs for compound **1** and **2** in below. Intramolecular O—H...O and intermolecular O—H...O hydrogen bonds are observed in **1** and **2**. In the crystalline architecture of **1** and **2**, intermolecular O—H...O hydrogen bonds link the molecules which form one-dimensional polymeric chain structure along the *c* axis (Fig. 2a and Fig. 3a). C—H...O intermolecular interaction also connect the molecules in the structures which form to 3D structure of **1** and **2** (Table 3). This polymeric networks lie in the *bc*-plane and stacks along to the *a*-axis for **1** (Fig. 2b) and they lie in the *ac*-plane and stacks along to the *b*-axis for **2** (Fig. 3b). Besides that intermolecular C—H... π contacts are also observed in the hydrogen-bonded assembly of **1** and **2** (Table 3).

3.2. FTIR spectroscopy

The IR spectra of **1** and **2** were analyzed in comparison with the ligand H₂L. The IR spectra of H₂L show a broad band in a region 3162 cm⁻¹ due to O—H stretching. Several weak peaks observed for **1** and **2** in the range 3064–2836 cm⁻¹ is likely to be due to the aromatic and aliphatic C—H stretches. The characteristic C=N stretching frequencies are 1613 and 1640 cm⁻¹ for **1** and **2**, respectively. The shift of this band towards lower frequency compared to the ligand H₂L (1643 cm⁻¹) indicates that the coordination of the imine nitrogen atom

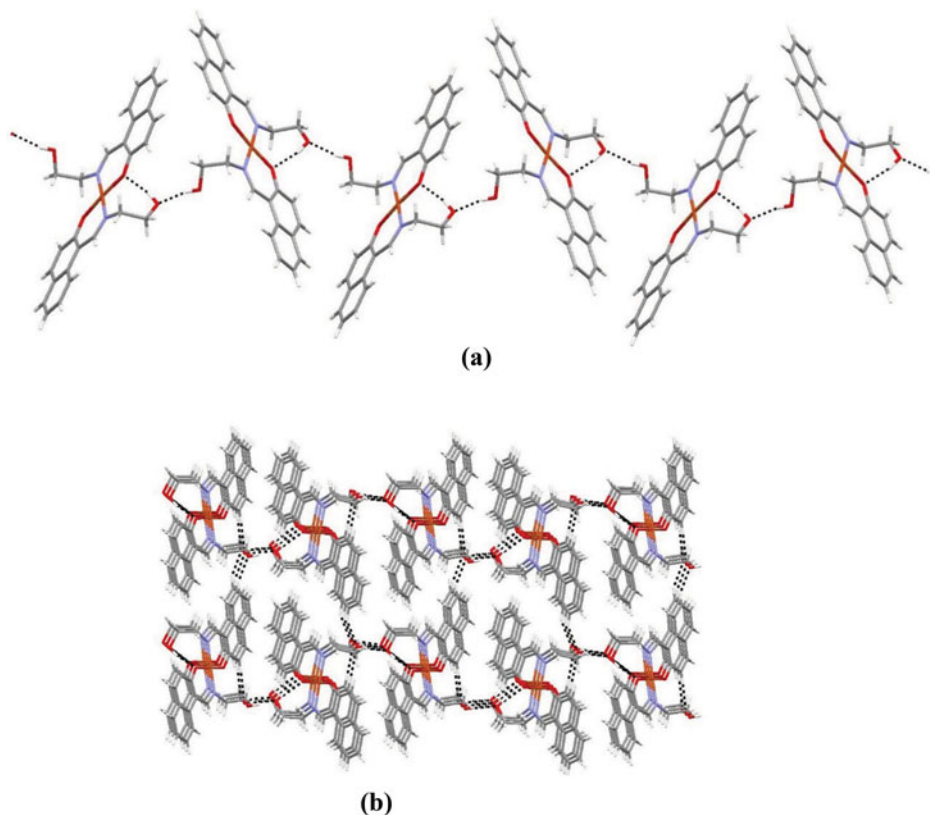
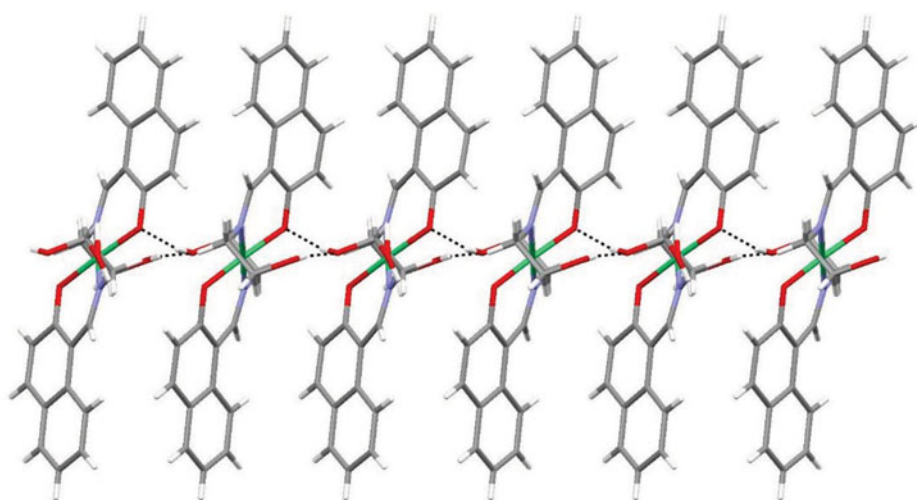


Figure 2. (a) O—H...O intermolecular interactions generating one-dimensional polymeric chain structure of **1** along the *c* axis. Dotted lines indicate hydrogen bonds. (b) C—H...O weak intermolecular interaction connect the molecules which form 3D structure.

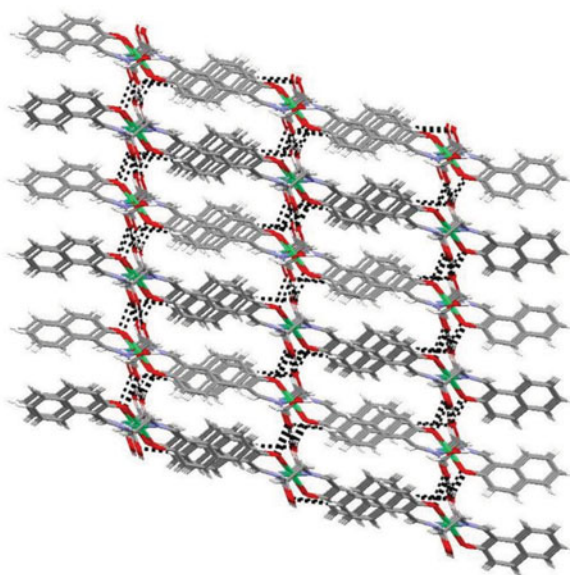
Table 3. Hydrogen bond geometry (Å, °) of compound **1** and **2**.

	D—H...A	D—H	H...A	D...A	D—H...A	Symmetry codes
1	O3—H3A...O4	0.84	1.92	2.741	167	1− <i>x</i> , 1/2+ <i>y</i>
	O4—H4...O2	0.84	1.83	2.657	167	
	C2—H2...O3	0.95	2.56	3.500	172	−1+ <i>x</i> , <i>y</i> , <i>z</i>
	C7—H7...O3	0.95	2.58	3.247	128	−1+ <i>x</i> , <i>y</i> , 1+ <i>z</i>
	C12—H12B...O2	0.99	2.39	2.845	107	
	C25—H25A...O1	0.99	2.32	2.790	108	
	C5—H5...Cg1	0.95	2.79	3.578	142	− <i>x</i> , 1/2+ <i>y</i> , 1− <i>z</i>
	C18—H18...Cg2	0.95	2.99	3.717	134	1− <i>x</i> , −1/2+ <i>y</i> , 1− <i>z</i>
2	O3—H3...O4A	0.84	2.03	2.862	173	<i>x</i> , 1− <i>y</i> , 1/2+ <i>z</i>
	O4A—H4B...O1	0.84	2.00	2.827	167	<i>x</i> , 1− <i>y</i> , −1/2+ <i>z</i>
	C6—H6...O3	0.95	2.55	3.465	161	1/2+ <i>x</i> , 1/2+ <i>y</i> , <i>z</i>
	C17—H17...O4A	0.95	2.59	3.486	158	−1/2+ <i>x</i> , −1/2+ <i>y</i> , <i>z</i>
	C23—H23B...O1	0.99	2.37	2.795	105	1− <i>x</i> , −1/2+ <i>y</i> , 1− <i>z</i>
	C23—H23B...O2	0.99	2.40	3.181	135	<i>x</i> , 1− <i>y</i> , 1/2+ <i>z</i>
	C24—H24A...O2	0.99	2.31	2.717	103	
	C24—H24A...O3	0.99	2.39	3.149	133	<i>x</i> , − <i>y</i> , −1/2+ <i>z</i>
	C25—H25B...O2	0.99	2.58	3.109	113	
	C19—H19...Cg3	0.95	2.85	3.743	156	−1/2+ <i>x</i> , 3/2− <i>y</i> , −1/2+ <i>z</i>

Cg1=C17—C18—C19—C20—C21—C22, Cg2=C1—C2—C3—C4—C9—C10, Cg3=C3—C4—C5—C6—C7—C8



(a)



(b)

Figure 3. (a) O—H...O intermolecular interactions generating one-dimensional polymeric chain structure of **2** along the *c* axis. Dotted lines indicate hydrogen bonds. (b) C—H...O weak intermolecular interaction connect the molecules which form 3D structure.

to the metal center [31]. The C—N single band stretching frequencies of **1** and **2** have been observed in the $1415\text{--}1342\text{ cm}^{-1}$ region [32]. The ligand coordination to the metal center is substantiated by bands appearing in the regions $558\text{--}473$ and $447\text{--}413\text{ cm}^{-1}$, attributable to $\nu(\text{M--N})$ and $\nu(\text{M--O})$, respectively, observed in complexes **1** and **2**. The infrared spectrum of complexes **1** and **2** are very much consistent with the structural data presented in this paper.

Table 4. Inhibition zones of the ligand **H₂L** and complexes **1** and **2** according to agar disc diffusion method [mm].

Microorganisms	Sources	H₂L	1	2	Standard
<i>Campylobacter jejuni</i>	ATCC 33291	7	8	7	10 ^C
<i>Enterobacter aerogenes</i>	NRRL 3567	8	9	10	9 ^C
<i>Escherichia coli</i>	ATCC 25292	9	10	10	11 ^C
<i>Listeria monocytogenes</i>	ATCC 7644	8	9	8	10 ^C
<i>Pseudomonas aeruginosa</i>	ATCC 27853	8	10	10	10 ^C
<i>Proteus vulgaris</i>	NRRL 123	8	9	10	10 ^C
<i>Staphylococcus aureus</i>	ATCC 6538	9	10	9	10 ^C
<i>Serratia marcescens</i>	clinical isolate	8	9	9	9 ^C
<i>Shigella sonnei</i>	ATCC 25931	8	9	9	9 ^C
<i>Klebsiella pneumoniae</i>	clinical isolate	8	9	9	9 ^C
<i>Candida albicans</i>	ATCC 10231	7	8	9	9 ^K
<i>Candida albicans</i>	clinical isolate	8	9	9	9 ^K

^C : Chloramphenicol (1000 µg/mL), ^K: Ketoconazole (1000 µg/mL)

3.3. Antibacterial and antifungal activity

The Schiff base ligand **H₂L** and its metal complexes **1** and **2** were evaluated for antimicrobial activity against the 10 bacteria, 2 yeast, 5 filamentous fungi. The antimicrobial activities are presented in [table 4](#) and [5](#), showing that the free ligand and both metal complexes exhibit antibacterial activity against all test bacteria and yeast strains. Antimicrobial inhibitions were compared with the activity of Chloramphenicol and Ketoconazole as a standard. The results of agar disk diffusion assay exhibit that **1** and **2** have high antimicrobial activity against *Pseudomonas aeruginosa*, *Escherichia coli*. **H₂L**, **1** and **2** effect bacteria and yeasts because they show clear inhibition zones with the tested bacteria and yeast on solid agar media. At the end of incubation, the diameters of the inhibition zones are in the range of 7–10 mm. The complex **1** is most effective against *Campylobacter jejuni*, *Pseudomonas aeruginosa*, *Staphylococcus aureus*, on the other hand the complex **2** is most effective against *Enterobacter aerogenes*. The complex **1** exhibited anticandidal activity with MIC value of 125 µg/mL. Metal complexes **1** and **2** exhibited higher activity than free ligand under identical experimental conditions ([Table 4](#) and [Table 5](#)). The metal salts used for the synthesis of complexes exhibit negligibly small antimicrobial activities [33,34]. Enhancement of activity of ligand after chelation can be explained on the basis of Overtones and Tweedy's concepts [35].

Table 5. Minimum Inhibitory Concentration [µg/mL] of the ligand **H₂L** and complexes **1** and **2**.

Microorganisms	Sources	H₂L	1	2	Standard
<i>Campylobacter jejuni</i>	ATCC 33291	250	125	250	250 ^C
<i>Enterobacter aerogenes</i>	NRRL 3567	500	250	125	250 ^C
<i>Escherichia coli</i>	ATCC 25292	250	125	125	125 ^C
<i>Listeria monocytogenes</i>	ATCC 7644	250	125	250	125 ^C
<i>Pseudomonas aeruginosa</i>	ATCC 27853	250	125	125	250 ^C
<i>Proteus vulgaris</i>	NRRL 123	500	250	125	125 ^C
<i>Staphylococcus aureus</i>	ATCC 6538	250	125	250	125 ^C
<i>Serratia marcescens</i>	clinical isolate	250	250	250	250 ^C
<i>Shigella sonnei</i>	ATCC 25931	500	250	250	250 ^C
<i>Klebsiella pneumoniae</i>	clinical isolate	500	250	250	250 ^C
<i>Candida albicans</i>	ATCC 10231	500	250	250	250 ^K
<i>Candida albicans</i>	clinical isolate	250	125	250	250 ^K

^C : Chloramphenicol (1000 µg/mL), ^K: Ketoconazole (1000 µg/mL)

Table 6. Antifungal activity data of the ligand **H₂L** and complexes **1** and **2** (Inhibition %).

Filamentous Fungi	H₂L	1	2	Ketoconazole
<i>Aspergillus flavus</i>	9.3	18.3	10.5	83.63
<i>Aspergillus niger</i>	15	29.7	16.6	40
<i>Penicillium expansum</i>	9.5	14.2	20.8	65
<i>Penicillium lanosum</i>	19	27.7	23	54
<i>Alternaria alternata</i>	9.2	11.1	14.2	82

Investigation of antifungal activity of the ligand **H₂L** and its metal complexes **1** and **2** revealed that both metal chelates are more toxic than the ligand (Table 6). The complex **1** is most effective against *Aspergillus flavus*, *Aspergillus niger*, *Penicillium lanosum*. On the other hand, *Penicillium expansum* and *Alternaria alternata* was more sensitive to complex **2**. *Aspergillus niger* was more sensitive (29.7%) against to both complexes.

The determination of structure–activity relationships implies that the biological activity of the products under examination should be evaluated using a very reliable assay. Previously we studied the antibacterial and antifungal activities of the ONO type Schiff base metal complexes [Ni(HL1)₂H₂O], [Fe(HL1)₂] [HL1 = *N*-(2-hydroxyethyl)-5-nitrosalicylaldimine] and [Co(HL2)(L2)] and [Co(HL3)(L3)] [HL2 = 2-((*E*)-(2-hydroxyethylimino)methyl)-4-chlorophenol and HL3 = 2-((*E*)-(2-hydroxyethylimino)methyl)-4-bromophenol]. The results showed that Schiff base metal complexes demonstrated antimicrobial activity against all tested micro-organisms and Ni(II), Fe(II) and Cu(II) complexes showed higher antibacterial and anticandidal activities than Co(III) complexes [10, 11]. The relation between chelation and toxicity is very complex, expected to be a function of steric, electronic, and pharmacokinetic factors along with mechanistic pathways [36]. Stability constants, solubility, particle size, size of metal ion, and magnetic moments may also be responsible for the antimicrobial activity of the complexes [37, 38]. Attempts to show a relationship between stability constants and antimicrobial activity of the complexes proved futile.

4. Conclusion

The tridentate Schiff base ligand (**H₂L**) and its metal complexes, [Cu(HL)₂], **1** and [Ni(HL)₂], **2** were synthesized and characterized. The crystal structures of complexes **1** and **2** have been determined by single crystal diffraction at 100 K. Single-crystal X-ray diffraction studies confirm that the metal center in complex **1** and **2** have distorted square planar. In the crystalline architecture of **1** and **2**, intermolecular O–H···O hydrogen bonds link the molecules which form one-dimensional polymeric chain structure along the *c* axis. This structures further stabilized by CH···O and C–H··· π stacking interactions. The Schiff base ligand **H₂L** and its metal complexes **1** and **2** were screened for the antibacterial and antifungal activities by the disc diffusion, microdilution broth and single spore culture techniques. The antimicrobial activities show that the ligand and both metal complexes exhibit antibacterial activity against all test bacteria and yeast strains. Metal complexes **1** and **2** exhibited higher activity than free ligand **H₂L** under identical experimental conditions.

Acknowledgments

The authors are grateful to the Scientific and Technological Research Council of Turkey (TUBITAK) (grant number TBAG-108T431) for the financial support. Dr. Kara would like to thank TUBITAK for

NATO-B1 and the Royal Society short visit fellowship for financial support and Prof. A. Guy Orpen (School of Chemistry, University of Bristol, UK) for his hospitality.

References

- [1] Zayed, E. M., & Zayed, M. A. (2015). *Spectrochim. Acta Part A*, 143, 81.
- [2] Ruanwas, P., Chantapromma, S., & Fun, H-K., (2015). *Mol. Cryst. Liq. Cryst.*, 609, 126.
- [3] Sanjeevarayappaa, C., Pushpa Iyengara, K. E. Kumar Manoj & Suchetan, P. A. (2015) *Mol. Cryst. Liq. Cryst.*, 607, 232.
- [4] Scozzafava, A., & Supuran, C. T. (2000). *J. Med. Chem.*, 43, 3677.
- [5] Shao, X., Ekstrand, D. H. L., Bhikhabhai, R., Kallander, C. F. R., & Gronowitz, J. S. (1997). *Antiviral Chem. Chemother.*, 8, 149.
- [6] Das, M., and Livingstone, S. E. (1976). *Inorg. Chim. Acta*, 19, 5.
- [7] Smith, H. J., & Simons, C. (2001). *Proteinase and Peptidase Inhibition: Recent Potential Targets for Drug Development*, Taylor and Francis, London.
- [8] Geeta, B., Shravan Kumar, K., Reddy, P. M., Ravikrishna, E., Sarangapani, M., Reddy K. K., Ravinder, V. (2010). *Spectrochim. Acta Part A*, 77, 911.
- [9] Kumar, G., Kumar, D., Devi, S., Johari, R., Singh, C. P. (2010). *Eur. J. Med. Chem.*, 45, 3056.
- [10] Gungor, E., Celen, S., Azaz, D., & Kara, H. (2012). *Spectrochim. Acta Part A*, 94, 216.
- [11] Celen, S., Gungor, E., Kara, H., & Azaz, A. D. (2013). *J. Coord. Chem.*, 66, 3170.
- [12] Azaz, A. D., Celen, S., Namli, H., Turhan, O., & Kurtaran, R. (2007). *Transition Met. Chem.*, 32, 884.
- [13] Namli, H., Azaz, A. D., Karabulut, S., Celen, S., & Kurtaran, R. (2007). *Transition Met. Chem.*, 32, 266.
- [14] Saha, N. C., Pradhan, R., Das, M., Khatun, N., Mitra, D., Samanta, A., Slawin, A. M. Z., Jana, A. D., Klanke, J., & Rentschler, E. (2014). *J. Coord. Chem.*, 67, 286.
- [15] Jadhavy, S. M., Shelkey, V. A., Munde A. S., Shankarwary, S. G., Patharkary, V. R. & Chondhekar, T. K., (2010) *J. Coord. Chem.* 63, 4153.
- [16] Liu, H. Y., Gao, F., Lu, Z. S., & Wang, H. Y. (2006). *Acta Cryst.*, E62, m1306.
- [17] Bruker-AXS SAINT V760A.
- [18] Sheldrick, G. M. (2008). SADABS V2008/1, University of Göttingen, Germany.
- [19] Sheldrick, G. M. (1999). SHELXTL Version 51, Program for the Solution and Refinement of Crystal Structures, Bruker AXS, Inc, Madison, WI, USA.
- [20] Flack, H. D. (1983). *Acta Crystallogr.*, A39, 876.
- [21] Parsons, S., Flack, H. D. & Wagner, T. (2013). *Acta Cryst.* B69, 249.
- [22] Farrugia, L. J. (2012). Ortep-3 for Windows. *J. Appl. Cryst.*, 45, 849.
- [23] CCDC. (2006). Mercury 2.3. Supplied with Cambridge Structural Database; CCDC: Cambridge, U.K.
- [24] NCCLS (National Committee for Clinical Laboratory Standards) (1997). *Performance Standards for Antimicrobial Disc Susceptibility Test*, sixth ed, Approved Standard, M2-A6, NCCLS, Wayne, PA.
- [25] Koneman, E. W., Allen, S. D., Janda, W. M., Srekenberger, P. C., & Winn, W. C. (1997). *Colour Atlas and Textbook of Diagnostic Microbiology*, Lippincott-Raven Publishers, Philadelphia, PA p785.
- [26] Hasenekoglu (1990). *Laboratory Techniques for Microfungi* Ataturk University, Erzurum, Turkey, p66.
- [27] Hadecek, F., & Greger H. (2000). *Phytochem. Anal.*, 11, 137.
- [28] Dharmaraj, N., Viswanathamurthi, P., & Natarajan, K. (2001). *Trans. Met. Chem.*, 26, 105.
- [29] Maniukiewicz, W., & Bukowska-Strzyzewska, M. (1990). *J. Crystallogr. Spectrosc. Res.*, 20, 363.
- [30] Midoes, A. C. D., Aranha, P. E., Dos Santos, M. P., Tozzo, E., Romera, S., Santos, R. H. A., & Dockal, E. R. (2008). *Polyhedron*, 27, 59.
- [31] Rahaman, S. H., Ghosh, R., Lu, T. H., & Ghosh, B. K. (2005). *Polyhedron*, 24, 1525.
- [32] Wang, X., Zang, X. M., & Lin, H. X. (1995). *Polyhedron*, 14, 293.
- [33] Jeragh, B. & El-Dissouky, A. (2005). *J. Coord. Chem.*, 12, 1029.
- [34] El-Dissouky, A., Al-Fulaji, O., Awad, M. K., & Rizk, S. (2010). *J. Coord. Chem.*, 63, 330.

- [35] Thangadurai, D. & Natarajan, K. (2001). *Synth. React. Inorg. Met.-Org. Chem.*, 30, 569.
- [36] Anaconda, J. R. & Acosta, F. (2005). *J. Coord. Chem.*, 59, 621.
- [37] El-Gamel, N. E. A. (2010). *J. Coord. Chem.*, 63, 534.
- [38] Nishat, N., Praveen, S. & DhyaniAsma, S. (2009). *J. Coord. Chem.*, 62, 1091.